CHEMISTRY OF MATERIALS

ARTICLE

pubs.acs.org/cm

Reductive Self-Assembling of Ag Nanoparticles on Germanium Nanowires and Their Application in Ultrasensitive Surface-Enhanced Raman Spectroscopy

Mingfa Peng,[†] Jing Gao,[†] Pingping Zhang,[†] Yang Li,[†] Xuhui Sun,[*,†] and Shuit-Tong Lee[*,‡]

[†]Institute of Functional Nano and Soft Materials (FUNSOM), and Jiangsu Key Laboratory for Carbon-Based Functional Materials and Devices, Soochow University, Suzhou, Jiangsu 215123, P. R. China

[‡]Center of Super Diamond and Advanced Materials (COSDAF), and Department of Physics and Materials Science, City University of Hong Kong, Kowloon, Hong Kong SAR, China

Supporting Information

ABSTRACT: Silver nanoparticles (AgNPs) have been reductively fabricated on the hydrogen-terminated surface of germanium nanowires (GeNWs), which exhibited moderate reactivity toward the direct reduction of Ag (I) ion to metal nanoparticles in aqueous solution at room temperature. The electronic properties of the AgNPs/GeNWs system have been studied by X-ray photoelectron spectroscopy. The Ag nanoparticle-embedded germanium nanowires have been used as a unique surface-enhanced Raman scattering substrate, which could achieve the single molecule detection. The observed enhancement factor of the fabricated AgNPs/GeNWs substrate was estimated to be 10^7.

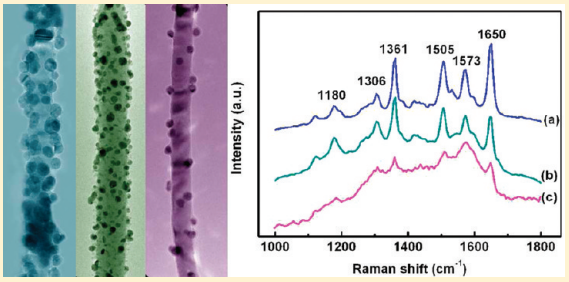

KEYWORDS: Ag nanoparticles, Ge nanowires, self-assembling, SERS

INTRODUCTION

In recent years, metal nanoparticles have attracted much attention due to their uses in a wide range of applications such as in catalysts,[1] surface-enhanced Raman scattering (SERS),[2] and biological applications (sensor, biological imaging, cancer therapy, etc).[3,4] In the past few years, many fabrication strategies such as colloidal chemistry and electrodeposition methods have been used to prepare metal nanoparticles such as Ag, Cu, Pt, Pd, and Au.[5,6] Recently, we reported the redox surface chemistry of Si nanowires (SiNWs) in connection with the fabrication of metallic nanostructures using a nanostructure template by studying the reaction of SiNWs with a number of metal ions such as Ag, Cu, Pd, Rh, Au, etc., in solution.[7−10] We found that the HF-etched SiNW surface is hydrogen-passivated and can readily reduce metal ions to metal nanostructures at room temperature, becoming reoxidized in the process, via the galvanic displacement reaction. These nanosystems generally exhibit electronic properties different from those of the bulk materials. By reductively depositing metal nanoparticles on the surfaces of SiNWs in solution at room temperature, we assembled these metal nanoparticles, which may be considered as zero-dimensional nanodots on one-dimensional nanowires.[11] It is believed that the fabrication of such metallic nanodots on semiconductor nanowires will eventually lead to new and novel composite materials of importance in nanotechnology, for example, as high-efficiency catalysts[12] and SERS substrates.[13−18] Compared with Si, Ge has gained renewed interest as a material of choice for future electronics and high-performance devices.[19] Because of their smaller effective mass, electrons and holes exhibit higher mobility in Ge than in Si, making Ge a better choice for high-performance logic computing. In addition, the larger exciton Bohr radius of Ge (24.3 nm) compared to that of Si (4.9 nm) allows for quantum confinement to be observed in relatively larger structures,[20,21] potentially useful for extremely low-power, high-speed quantum computing. Also, Ge nanowires offer the advantage of lower growth temperature compared to that of Si nanowires, making their direct integration into nanochip fabrication much easier.[22] While several successful synthetic strategies have been studied to prepare high-quality germanium nanowires, such as laser ablation,[23] vapor transport,[24,25] chemical vapor deposition (CVD),[26] and supercritical fluid-liquid−solid (SFLS),[27] information on the surface properties of GeNWs is relatively lacking,[28−30] especially surface chemical reactivity properties.

In this article, we studied the chemical reactivity of GeNWs through the redox reaction process on GeNW surface in aqueous solution using Ag ions as a sample. The oxide outer layer of the as-prepared GeNWs can be easily removed by a HF treatment. Ag nanoparticles have been self-assembled on the surface of

Received: January 19, 2011
Revised: May 13, 2011
Published: June 28, 2011

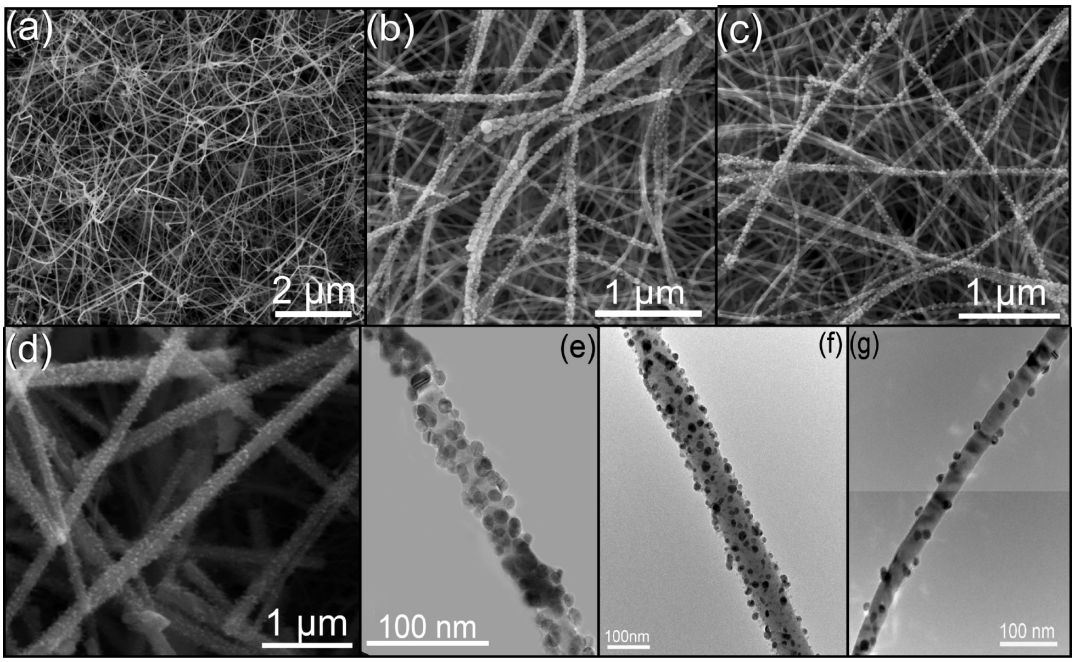

Figure 1. SEM images of (a) as-prepared GeNWs and (b−d) Ag nanoparticles on GeNWs, formed in 10^{-3} M, 10^{-4} M, and 10^{-5} M Ag (I) solution, respectively. (e−g) TEM images of AgNPs on GeNW formed in 10^{-3} M, 10^{-4} M, and 10^{-5} M Ag (I) solution, respectively.

HF-etched GeNWs at room temperature. Although the redox process of GeNWs is similar to that of SiNWs, the difference in morphology and structure of the formed products between GeNWs and SiNWs was observed due to the higher surface reactivity of Ge and much lower stability of Ge oxide in aqueous solution than those of Si. The electronic properties of AgNPs and GeNWs have been studied by X-ray photoelectron spectroscopy (XPS). The as-prepared AgNPs/GeNWs can be applicable as an ultrasensitive SERS substrate.

EXPERIMENTAL SECTION

GeNWs used in this work were prepared by the thermal evaporation method under the vapor−liquid−solid (VLS) mechanism as described previously.[25] In brief, GeNWs have been synthesized by the thermal evaporation of Ge powder at 950 °C and then deposited onto the Si wafer substrate at ∼600 °C using Au nanoparticles as catalysts. Figure 1 (a) shows the scanning electron microscopy (SEM) image of as-prepared GeNWs of several micrometers in length with high density. Under transmission electron microscopy (TEM) imaging (see Figure S1a in the Supporting Information), the as-prepared GeNWs have a crystalline core of ∼50 nm on average, which is coated by a thin layer germanium oxide (the thickness is about 5 nm). The oxide layer was removed by immersing the as-prepared GeNWs into a 5% HF aqueous solution for 2 min (Figure S1b, Supporting Information). The HF-etched GeNWs were rinsed with deionized water and then immediately immersed in silver(I) nitrate aqueous solutions with different concentrations (10^{-3} M, 10^{-4} M, and 10^{-5} M) for one minute. After the reaction, the treated GeNWs were rinsed in deionized water and dried immediately by N_2 blow and transferred into a vacuum chamber for further measurements.

The morphology and structure of the products were first characterized by SEM (FEI Quanta FRG 200F) and high-resolution TEM (HRTEM) (FEI Tecnai G2 F20 S-TIWN). The surface state of the as-synthesized products was obtained by XPS measurement (Kratos AXIS Ultra^{DLD} ultrahigh vacuum (UHV) surface analysis system), using Al Kα radiation (1486 eV) as a probe. An electron flood gun was used for all measurements to compensate charging, and final spectra were calibrated to the adventitious carbon C 1s peak at 284.6 eV. Survey and high-resolution spectra were recorded at 80 and 20 eV pass energies, respectively, with an energy resolution of 0.5 at 20 eV pass energy. A Lab RAM HR 800 Raman microscope was used to carry out the SERS measurements, and the as-prepared AgNPs/GeNWs were used as SERS substrates. R6G was chosen as a model analyte to investigate the performance of the AgNPs-coated GeNWs as a substrate for SERS detection because R6G is extensively studied and well characterized by SERS.[31,32] The SERS measurements were performed by dropping 10 μL of R6G methanol solution of different concentrations (from 10^{-2} M to 10^{-16} M) onto the substrates. An argon ion laser of 514.5 nm at a spectral resolution of 1 cm^{-1} and a spot size of 1 μm was used for excitation. The laser power on the specimens was measured at 4 mW. The recorded spectra were raw data without any background subtraction or processing. The mapping function was applied to measure the SERS signal when the concentration of R6G is below 10^{-13} M. The mapping size used in the experiment is 100 × 80 μm^2, and the scan rate is set at 1 s/spectrum.

RESULTS AND DISCUSSION

It is well known that the as-prepared GeNWs have an oxide outer-layer due to oxidation of the GeNWs during or after growth. The oxide layer can be removed by a dilute HF aqueous solution. The HF-etched GeNWs were passivated by hydrogen, forming GeH_x on the surface of GeNWs.[30] The hydrogen-terminated GeNW (H-GeNW) is a modest reducing agent in aqueous solution. The H-GeNWs can readily reduce metal ions to nanoparticles on the surface of GeNWs at room temperature, serving both as a reducing agent and a nanotemplate substrate. In this process, the HF-etched GeNW surface is reoxidized to form GeO_x, but GeO_x can dissolve in the water to form $Ge(OH)_4$, which may facilitate the total redox reaction. Although a plausible reaction mechanism can be deduced from the reaction products, the reaction between H-GeNWs and metal ions in solution is a complex surface electrochemistry process. We propose the oxidation−reduction half reactions in the Ag-GeNWs system shown in Scheme 1.

dx.doi.org/10.1021/cm200186v |*Chem. Mater.* 2011, 23, 3296–3301

Scheme 1. Oxidation−Reduction Half Reactions in a Ag-GeNW System

Oxidation: $GeH_x + H_2O \longrightarrow GeO_2 + (x/2)H_2O + 4H^+ + 4e^-$ (1)

$Ge + H_2O \longrightarrow GeO_2 + 4H^+ + 4e^-$ (2) $\varphi^\theta = 0.15$ V

Reduction: $Ag^+ + e^- \longrightarrow Ag$ (3) $\varphi^\theta = 0.80$ V

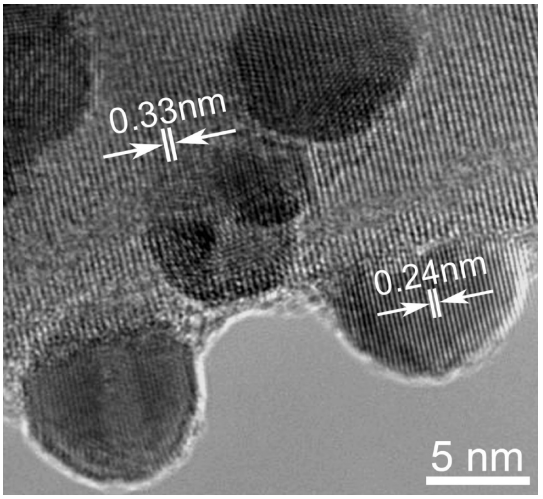

Figure 2. HR-TEM image of GeNWs treated by a 10^{-4} M silver(I) nitrate solution.

Since the surface GeH_x ($x = 1-3$) species is consumed quickly following the half reaction (eq 1), we believe that the Ge is the main reducing source for metal nanoparticle formation (half reaction eq 2). The standard potential of half reaction 2 is 0.15 V, and after considering the reaction happens in neutral medium with pH = 7, the potential of half reaction 2 changes to −0.26 V according to the Nernst equation. The potentials of half reaction 3 are 0.62, 0.56, and 0.50 V for Ag^+ concentrations of 10^{-3}, 10^{-4}, and 10^{-5} M, respectively. The lower the potential, the easier it is for the reactant to lose electrons and be oxidized. Compared to the potential of the half reaction of Si to SiO_2, 0.44 V at pH 7, GeNWs have a lower potential to reduce metal ions, such as Ag^+, Cu^{2+}, Au^{3+}, etc., ions to metal. The SEM images with EDS results of 10^{-3} M $HAuCl_4$ and $Cu(NO_3)_2$ aqueous solution treated GeNWs are shown Figure S2 in the Supporting Information.

The products from the reaction of HF-etched GeNWs and silver(I) nitrate of different concentrations are shown in Figure 1. It is observed that for all three Ag^+ concentrations, high-density Ag nanoparticles were formed on the surface of GeNWs. The density of AgNPs increased with increasing Ag^+ concentration, while the particle size decreased with decreasing Ag^+ concentration. The coverage percentages of AgNPs from 10^{-3} M, 10^{-4} M, and 10^{-5} M $AgNO_3$ on the GeNWs surface are estimated to 70%, 30% and 8%, respectively, by using contrasted image treatments followed by statistical measurements. The average sizes of AgNPs are 5, 10, and 15 nm for 10^{-5} M, 10^{-4} M, and 10^{-3} M Ag^+ concentration, respectively. The detailed structures of the AgNPs/GeNW were imaged by HRTEM as depicted in Figure 2, which shows the typical structure of the AgNPs/GeNW treated by 10^{-4} M Ag^+ solution. The HRTEM images of 10^{-3} M and 10^{-5} M Ag^+ solution treated GeNW are shown in Figure S3 (Supporting Information). These nanoparticles have a lattice

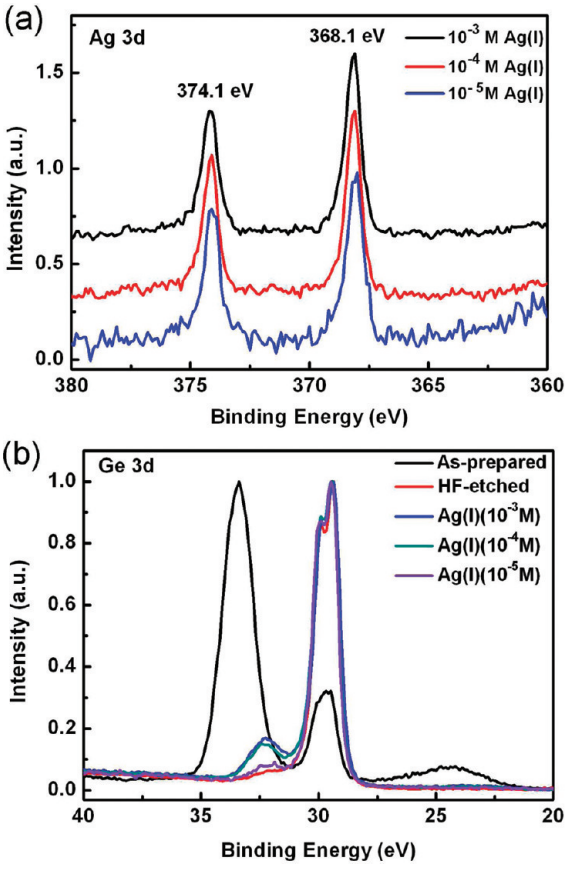

Figure 3. XPS spectra of (a) Ag 3d XPS spectra of GeNWs treated in different concentrations (10^{-3}, 10^{-4}, and 10^{-5} M) of silver nitrate, (b) Ge 3d XPS of the as-prepared and HF-etched GeNWs, and GeNWs treated in different concentrations (10^{-3} M, 10^{-4} M, and 10^{-5} M) of silver nitrate.

spacing of 0.24 nm indicating that the particles are crystalline Ag with a face-centered cubic (fcc) structure, and the GeNWs have a 0.33 nm spacing of Ge (111) planes. Compared to the AgNP/SiNW system,[7] the AgNP/GeNW shows two distinct features. First, the metal nanoparticles are directly attached to the GeNW surface with no interfacial oxide, while in AgNPs/SiNWs, Ag nanoparticles were attached to or embedded in Si oxide. Second, the density of metal nanoparticles on GeNWs is much larger than that on SiNWs. These differences are attributed to the differences in surface reactivity of Ge and Si and stability of their oxide in water.

Detailed information about the surface electronic structure of the obtained AgNPs/GeNWs was provided by the XPS analysis. Figure 3a shows the XPS spectra of Ag 3d of the AgNPs, from the different concentrations (10^{-3}, 10^{-4}, and 10^{-5} M). For GeNWs treated in different concentrations, the XPS spectra are similar, except that the signal-to-noise ratio decreases slightly with decreasing concentration of the metal ion solutions, due to the formation of smaller amount of nanoparticles (low density and small size of AgNPs) in the lower concentration solution. The binding energies of Ag $3d_{5/2}$ and Ag $3d_{3/2}$ are detected at 368.1 and 374.1 eV, respectively, which are well consistent with those of Ag metal, confirming that they are Ag nanoparticles on the surface of GeNWs. Figure 3b records the evolution of the Ge 3d electronic state versus Ag ion solutions. In the Ge 3d region of the as-prepared GeNWs, there is an intense peak (33.2 eV) at ∼3.6 eV above the

dx.doi.org/10.1021/cm200186v |*Chem. Mater.* 2011, 23, 3296–3301

binding energy of the Ge 3d (a broad peak centered at 29.6 eV). It has been established that surface Ge can be readily oxidized by electronegative elements through several oxidation states (1−4), and the binding energy increase associated with an unit increase in oxidation state (i.e., per Ge−O bond) is ∼0.85 eV.[33] The intense peak is thus attributed to GeO_2 on the outer layer of the GeNWs. In addition, there is a broad peak centered at 24 eV, which is the O 2s peak of oxygen in GeO_2. After HF etching, the oxide peaks disappear, and the Ge 3d peak exhibits a $3d_{3/2}$ and $3d_{5/2}$ spin−orbit splitting of 0.58 eV. This further confirms that the GeO_2 outer layer was clearly removed by HF etching. After immersing into silver nitrate solutions, a broad suboxide peak centered at 32.2 eV appears at slightly lower binding energy than GeO_2, representing Ge^{3+} with little Ge^{2+} and Ge^{+} oxidation states. It was found that the surface of GeNWs can only be oxidized to Ge^{3+} under atmospheric conditions and could be oxidized to Ge^{4+} under UV irradiation.[34] As Ag^{+} concentration increases, the intensity of the oxide peak slightly increases, but unlike the case of AgNPs/SiNWs, where the Si oxide peak exhibited a significant increase with increasing Ag^{+} concentration. We suppose that surface Ge atoms and Ge-hydrogen bonds in the etched GeNWs were oxidized by the silver ion in the solution; thus, the Ge surface was oxidized again, and oxidation would be more extensive with increasing Ag^{+} concentration. Since Ge oxide is water-soluble and can dissolve in the solution immediately after formation, consequently little surface oxide was left and detected by XPS, and no apparent oxide was observed in HRTEM image.

AgNPs have been widely used as the SERS source due to their strong SERS activity.[35−37] SERS has become a powerful technique to detect chemical and biological molecules toward single-molecule detection sensitivity. There are some reports about silver nanoparticles coated on SiNWs surface as the SERS substrate.[13,14,35−37] Here, GeNWs coated with Ag nanoparticles were used as SERS substrates to detect Rhodamine 6G (R6G), a typical model analyte for SERS performance evaluation, and shown to be ultrasensitive SERS substrates. There is no enhancement effect on the GeNWs without Ag nanoparticles. The GeNW substrate displays very weak Raman signals for a 10^{-3} M R6G aqueous solution, with a detection limit of only $\sim 10^{-4}$ M. According to the electromagnetic theory of SERS, the size, shape, and proximity of nanostructures all affect the frequency and magnitude of the localized surface plasmons, i.e., the degree of Raman enhancement.[38] The characteristics of Ag nanoparticles, i.e., size, separation, and high density, coated on GeNWs may provide an optimum environment for the enhancement in Raman signals. The three different AgNP/GeNW substrates from three concentrations of Ag^{+} solution (10^{-3}, 10^{-4} ,and 10^{-5} M) treated GeNWs were applied in the SERS test using 10 μL 10^{-8} M R6G as the probe. The results are shown in Figure 4a. Prominent Raman bands of R6G at 1650, 1572, 1505, 1361, 1306, and 1180 cm^{-1} are observed in Figure 4a. The peak at 1180 cm^{-1} is associated with C−C in-plane bend modes, and the signals between 1306 and 1650 cm^{-1} are due to aromatic C−C stretching vibrations.[39] We found that 10^{-3} M Ag^{+} treated GeNWs exhibit the best performance in the SERS tests probably due to the optimized size, separation, and density of AgNPs on GeNWs. The 10^{-3} M Ag^{+} treated GeNWs have high density AgNPs with 70% coverage on GeNWs, and the diameter of AgNPs is around 15 nm, which is the optimum size for SERS.[38,40] Figure 4b shows the corresponding SERS spectra on the 10^{-3} M AgNP/GeNW substrates for R6G of different concentrations.

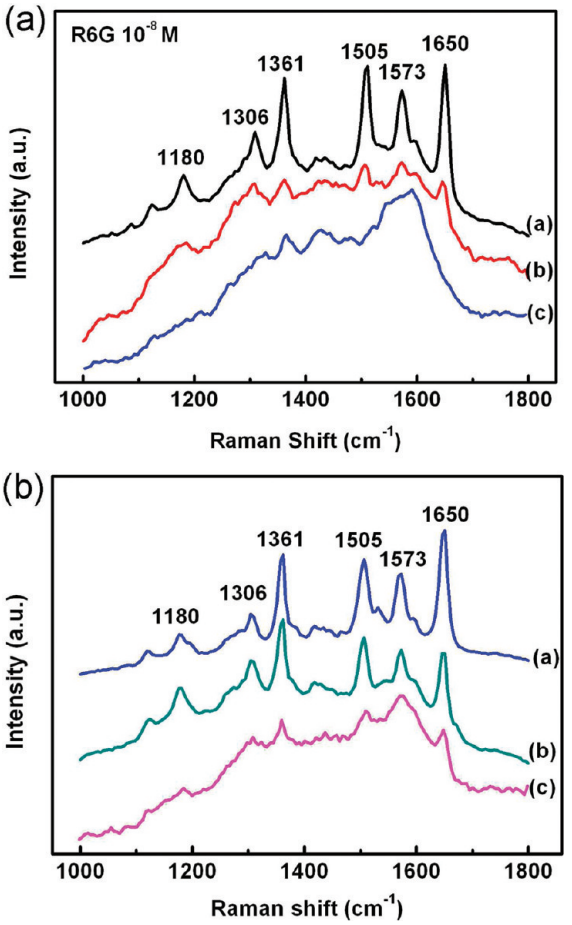

Figure 4. (a) SERS spectra of 10 μL 10^{-8} M R6G on (a) 10^{-3} M, (b) 10^{-4} M, and (c) 10^{-5} M $AgNO_3$ treated GeNWs substrates. (b) SERS spectra obtained from AgNPs-coated GeNWs treated with 10 μL of R6G solution of different concentrations. (a) 10^{-13} M R6G, (b) 10^{-15} M R6G, and (c) 10^{-16} M R6G.

When the amount of R6G on the AgNP/GeNW substrate (5 mm^2 in area) was reduced to 10^{-16} M (10 μL solution contains about 602 molecules), there are about 8 R6G molecules in the mapping size (100 × 80 μm^2). The peak of R6G molecules were still observed as shown in curve c, which contains the same characteristic Raman peaks of R6G in common with curves a and b. This indicates that the AgNPs/GeNWs substrate is promising for probing single molecules due to its high surface enhancement efficiency.

Localized surface plasmon resonance (LSPR) makes a major contribution to the electromagnetic field enhancement and therefore SERS. The LSPR strength and frequency are influenced by the incident laser wavelength, the morphology of the substrate, and the surrounding medium.[41−43] In order to investigate the LSPR effect in AgNPs/GeNWs substrate, the extinction spectrum of AgNPs (10^{-3} M) /GeNWs was recorded by UV−vis spectroscopy, as shown in Figure S6 (Supporting Information). Generally, the AgNPs dispersed in solution or formed in 2-D films have one isolated plasmon peak in their extinction spectra, and the peak position and shape are dependent on the size, shape, arrangement (e.g., density and interparticle spacing), and the surrounding dielectric constant of AgNPs.[44−46] In our case, the AgNPs are distributed on a 3-D GeNW network with high

dx.doi.org/10.1021/cm200186v |Chem. Mater. 2011, 23, 3296–3301

density and reduced interparticle spacing, and the dipoles induced by plasmon resonance would couple and transmit on the whole surface. Consequently, the plasmon resonance absorption of our substrate is broad and strong, which is an evidence for the high enhancement effect of the AgNPs/GeNWs substrate.

Significantly, the SERS result on AgNPs/GeNWs is better than that on AgNP/SiNW substrate whose detection limit is 1500 molecules.[13] It may be due to the absence of oxide between AgNPs and GeNWs or that on AgNPs because oxide may adversely affect surface plasmon resonance. In addition to electromagnetic enhancement, the chemical enhancement involving an enhanced scattering process associated with chemical interaction between the molecule and the SERS surface may contribute to the total enhancement. AgNPs were directly deposited on crystalline Ge nanowires, and the surfaces of AgNPs are completely free of organic contaminations and oxidation. The clean surface of AgNPs would expose more active centers for interactions with dye molecules, thus additionally increasing the chemical enhancement effect. The detailed mechanism needs to be further investigated.

Raman enhancement factor (EF) can be estimated from the experiments as follows:[47,48]

$$\mathrm{EF} = \frac{I_{SERS}/N_{Surf}}{I_{RS}/N_{Vol}}$$

where I_{SERS} and I_{RS} are the Raman intensity of the same Raman band under SERS and normal Raman conditions, respectively. N_{Surf} and N_{Vol} are the number of molecules on the SERS substrate and that in bulk illuminated by the laser focus spot, respectively. Here, the two strongest Raman bands at 1650 cm^{-1} and 1361 cm^{-1} are selected to calculate the EF.[49] During the experiment, the Raman measurement parameters including the laser power were kept constant. The I_{RS} was obtained from 10^{-3} M R6G solution on a GeNWs sample. The I_{SERS} could be obtained from 10^{-9} M R6G on the AgNP/GeNW sample. N_{Vol} values were estimated by considering the laser spot scattering volume to be 2.1×10^6 molecules, and N_{Surf} values are primarily determined by the number of R6G on the surface of AgNPs in the scattering volume. N_{Surf} = 0.74 molecule was determined. Detailed calculations can be found in the Supporting Information. Note that this value, which is lower than one molecule in the confocal volume, is still sufficient to record a Raman signal. This can be explained by the molecular migration during acquisition due to Brownian motion and/or the adsorption of R6G molecules on the AgNPs.[50,51] On the basis of calculations, the EF value of the AgNP/GeNW substrate is 3.8×10^7 and 4.3×10^7, respectively, depending on the choice of the Raman peaks. The EF of the AgNP/GeNW substrate estimated to be 10^7 and 10^{-9} M R6G is already in the single molecule detection range.[52]

CONCLUSIONS

Silver nanoparticles with a small diameter and high density have been self-assembled on the hydrogen-terminated surfaces of GeNWs, which play a key role in the reduction of Ag (I) ion to metal nanoparticles in aqueous solution at room temperature. The AgNPs are well-defined single crystals and directly attached to the surface of GeNWs due to the dissolution of formed Ge oxide in water. The GeNW surface shows a much higher reactivity than the SiNW surface in the redox process. The Ag nanoparticle-embedded GeNWs have been used as unique SERS substrates, which can detect 10^{-16} M R6G in methanol solutions. The enhancement factor of the AgNP/GeNW substrate was estimated to be 10^7.

ASSOCIATED CONTENT

Supporting Information. HRTEM images of as-prepared, HF-etched and $AgNO_3$ (10^{-3} and 10^{-5} M) treated GeNWs; SEM images and corresponding EDS of Au nanoparticles on GeNWs formed in 10^{-3} M $HAuCl_4$ solution and Cu nanoparticles on GeNWs formed in 10^{-3} M $CuSO_4$ solution; detailed calculation of the SERS enhancement factor (EF); Raman intensity-depth profile of the integrated intensity of 520 cm^{-1} band for a Si wafer to determine the effective height of the scattering volume (H_{eff}); SERS of 10 μL 10^{-9} M R6G on 10^{-3} M $AgNO_3$ treated GeNWs substrates; and UV−vis extinction spectrum of AgNPs on GeNWs formed in 10^{-3} M $AgNO_3$ solution (PDF). This material is available free of charge via the Internet at http://pubs.acs.org.

AUTHOR INFORMATION

Corresponding Author

*E-mail: xhsun@suda.edu.cn (X.S.); apannale@cityu.edu.hk (S.-T.L).

ACKNOWLEDGMENT

We thank the experimental support from Junjun Zhu (TEM), Xiaoye Chen, and HuaixinWei (XPS). The work was supported by the National Basic Research Program of China (973 Program) (Grant No. 2010CB934502), Natural Science Foundation of China (NSFC) (Grant No. 51072127), the Priority Academic Program Development of Jiangsu Higher Education Institutions and the Science and Research Grants Council of HKSAR (CityU5/CRF/08 and CityU108/08).

REFERENCES

(1) Xie, X.; Li, Y.; Liu, Z. Q.; Haruta, M.; Shen, W. *Nature* **2009**, *458*, 746–749.
(2) Wang, X. T.; Shi, W. S.; She, G. W.; Mu, L. X.; Lee, S. T. *Appl. Phys. Lett.* **2010**, *96*, 053104.
(3) Tkachenko, A. G.; Xie, H.; Coleman, D.; Glomm, W.; Ryan, J.; Anderson, M. F.; Franzen, S.; Feldheim, D. L. *J. Am. Chem. Soc.* **2003**, *125*, 4700–4701.
(4) Ray, P. C. *Chem. Rev.* **2010**, *110*, 5332–5365.
(5) Chen, S.; Sommers, J. M. *J. Phys. Chem. B* **2001**, *105*, 8816–8820.
(6) Zhang, P.; Sham, T. K. *Phys. Rev. Lett.* **2003**, *90*, 245502–245504.
(7) Sun, X. H.; Sammynaiken, R.; Naftel, S. J.; Tang, Y. H.; Zhang, P.; Kim, P. S.; Sham, T. K.; Fan, X. H.; Zhang, Y. F.; Lee, C. S.; Lee, S. T.; Wong, N. B.; Hu, Y. F.; Tan, K. H. *Chem. Mater.* **2002**, *14*, 2519–2526.
(8) Sun, X. H.; Wong, N. B.; Li, C. P.; Lee, S. T.; Kim, P. S. G.; Sham, T. K. *Chem. Mater.* **2004**, *16*, 1143–1152.
(9) Sun, X. H.; Li, C. P.; Wong, N. B.; Lee, C. S.; Lee, S. T.; Teo, B K. *Inorg. Chem.* **2002**, *41*, 4331–4336.
(10) Sun, X. H.; Peng, H. Y.; Tang, Y. H.; Shi, W. S.; Wong, N. B.; Lee, C. S.; Lee, S. T.; Sham, T. K. *J. Appl. Phys.* **2001**, *89*, 6396.
(11) Teo, B. K.; Sun, X. H. *Chem. Rev.* **2007**, *107*, 1454–1532.
(12) Tsang, C. H. A.; Liu, Y.; Kang, Z. H.; Ma, D. D. D.; Wong, N. B.; Lee, S. T. *Chem. Commun.* **2009**, 5829–5832.
(13) Shao, M. W.; Zhang, M. L.; Wong, N. B.; Ma, D. D. D.; Wang, H.; Chen, W. W.; Lee, S. T. *Appl. Phys. Lett.* **2008**, *93*, 233118.
(14) Zhang, M. L.; Fan, X.; Zhou, X. W.; Shao, M. W.; Zapien, J. A.; Wong, N. B.; Lee, S. T. *J. Phys. Chem. C* **2010**, *114*, 1969–1975.
(15) Brejna, P. R.; Griffiths, P. R.; Yang, J. *Appl. Spectrosc.* **2009**, *63*, 396–400.

(16) Khan, M. A.; Hogan, T. P.; Shanker, B. *J. Raman. Spectrosc.* **2008**, *39*, 893–900.
(17) Yang, L. B.; Ma, L. A.; Chen, G. Y.; Liu, J. H.; Tian, Z. Q. *Chem. Eur. J.* **2010**, *16*, 12683–12693.
(18) Sivakov, V. A.; Hoflich, K.; Becker, M.; Berger., A.; Stelzner., T.; Elers, K. E.; Pore, V.; Ritala, M.; Christiansen, S. H. *ChemPhysChem* **2010**, *11*, 1995–2000.
(19) Wang, D. W.; Wang, Q.; Javey, A.; Tu, R.; Dai, H. J.; Kim, H.; McIntyre, P. C.; Krishnamohan, T.; Saraswat, K. C. *Appl. Phys. Lett.* **2003**, *83*, 2432.
(20) Maeda, Y.; Tsukamoto, N.; Yazawa, Y.; Kanemitsu, Y.; Masu-moto, Y. *Appl. Phys. Lett.* **1991**, *59*, 3168.
(21) Cullis, A. G.; Canham, L. T.; Calcott., P. D. J. *J. Appl. Phys.* **1997**, *82*, 909.
(22) Kamins, T. I.; Li, X.; Williams, R. S.; Liu, X. *Nano Lett.* **2004**, *4*, 503–506.
(23) Morales, A. M.; Lieber, C. M. *Science* **1998**, *279*, 208–211.
(24) Nguyen, P.; Ng, H. T.; Meyyappan, M. *Adv. Mater.* **2005**, *17*, 549–553.
(25) (a) Sun, X. H.; Didycguk, C.; Sham, T. K.; Wong, N. B. *Nanotechnology* **2006**, *17*, 2925–2930. (b) Sun, X. H.; Calebotta, G.; Yu, B.; Selvaduray, G.; Meyyappan, M. *J. Vac. Sci. Technol., B* **2007**, *25*, 415.
(26) Wang, D. W.; Dai, H. J. *Angew. Chem., Int. Ed.* **2002**, *41*, 4783–4786.
(27) Hanrath, T.; Korgel, B. A. *Adv. Mater.* **2003**, *15*, 437–440.
(28) Wang, D. W.; Chang, Y. L.; Wang, Q.; Cao, J.; Farmer, D. B.; Gordon, R. G.; Dai, H. J. *J. Am. Chem. Soc.* **2004**, *126*, 11602–11611.
(29) Wang, D. W.; Chang, Y. L.; Liu, Z.; Dai, H. J. *J. Am. Chem. Soc.* **2005**, *127*, 11871–11875.
(30) Hanrath, T.; Korgel, B. A. *J. Am. Chem. Soc.* **2004**, *126*, 15466–15472.
(31) Nie, S.; Emory, S. R. *Science* **1997**, *275*, 1102.
(32) Lin, H. H.; Mock, J.; Smith, D.; Gao, T.; Sailor, M. J. *J. Phys. Chem. B* **2004**, *108*, 11654.
(33) Schmeisser, D.; Schnell, R. D.; Bogen, A.; Himpsel, F. J.; Rieger, D.; Landgren, G.; Morar, J. F. *Surf. Sci.* **1986**, *172*, 455–465.
(34) Adhikari, H.; McIntyre, P. C.; Sun, S. Y.; Pianetta, P.; Chidsey, C. E. D. *Appl. Phys. Lett.* **2005**, *87*, 263109.
(35) He, Y.; Su, S.; Xu, T. T.; Zhong, Y. L.; Zapien, J. A.; Li, J.; Fan, C. H.; Lee, S. T. *Nano Today* **2011**, *6*, 122–130.
(36) Fang, C.; Agarwal, A.; Ji, H.; Karen, W. Y.; Yobas, L. *Nanotechnology* **2009**, *20*, 405604.
(37) Qiu, T.; Wu, X. L.; Shen, J. C.; Ha, P. C. T.; Chu, P. K. *Nanotechnology* **2006**, *17*, 5769–5772.
(38) Garcia-Vidal, F. J.; Pendry, J. B. *Phys. Rev. Lett.* **1996**, *77*, 1163.
(39) Hildebrandt, P.; Stockburger, M. *J. Phys. Chem.* **1984**, *88*, 5935–5944.
(40) Shao, M. W.; Lu, L.; Wang, H.; Wang, S.; Zhang, M. L.; Ma, D. D. D.; Lee, S. T. *Chem. Commun.* **2008**, 2310–2312.
(41) Hulteen, J. C.; Van Duynea, R. P. *J. Vac. Sci. Technol., A* **1995**, *13*, 1553–1558.
(42) Willets, K. A.; Van Duyne, R. P. *Annu. Rev. Phys. Chem.* **2007**, *58*, 267–297.
(43) Mulvihill, M. J.; Carraro, C.; Maboudian, R. *J. Am. Chem. Soc.* **2010**, *132*, 1476–1477.
(44) Anker, J. N.; Hall, W. P.; Lyandres, O.; Shah, N. C.; Zhao, J.; Van Duyne, R. P. *Nat. Mater.* **2008**, *7*, 442.
(45) Sai, V. V. R.; Gangadean, D.; Niraula, I.; Jabal, J. M. F.; Corti, G.; McIlroy, D. N. D.; Aston, E.; Branen, J. R.; Hrdlicka, P. J. *J. Phys. Chem. C* **2011**, *115*, 453–459.
(46) Mulvihill, M. J.; Ling, X. Y.; Henzie, J.; Yang, P. D. *J. Am. Chem. Soc.* **2010**, *132*, 268–274.
(47) Tian, Z. Q.; Gao, S. J.; Li, X. Q.; Ren, B.; Huang, Q. J.; Cai, W. B.; Liu, F. M.; Mao, B. W. *J. Raman. Spectrosc.* **1998**, *29*, 703.
(48) Le Ru, E. C.; Blackie, E.; Meyer, M.; Etchegoin, P. G. *J. Phys. Chem. C* **2007**, *111*, 13794–13803.
(49) Abdelsalam, M. E.; Mahajan, S.; Bartlett, P. N.; Baumberg, J. J.; Russell, A. E. *J. Am. Chem. Soc.* **2007**, *129*, 7399–7406.
(50) Galopin, E.; Barbillat, J.; Coffinier, Y.; Szunerits, S.; Patriarche, G.; Boukherroub, R. *ACS Appl. Mater. Int.* **2009**, *1*, 1396–1403.
(51) Sabur, A.; Havel, M.; Gogotsi, Y. *J. Raman. Spectrosc.* **2008**, *39*, 61–67.
(52) Tong, L. M.; Zhu, T.; Liu, Z. F. *Chem. Soc. Rev.* **2011**, *40*, 1296–1304.